Available online at www.sciencedirect.com

ScienceDirect

Geochimica et Cosmochimica Acta 308 (2021) 188–203

Geochimica et Cosmochimica Acta

www.elsevier.com/locate/gca

Biogeochemical influences on net methylmercury formation proxies along a peatland chronosequence

Baolin Wang [a], Shunqing Zhong [b,a,*], Kevin Bishop [a], Mats B. Nilsson [c], Haiyan Hu [d,a], Karin Eklöf [a], Andrea G. Bravo [e], Staffan Åkerblom [a], Stefan Bertilsson [a], Erik Björn [f], Ulf Skyllberg [c]

[a] Department of Aquatic Sciences and Assessment, Swedish University of Agricultural Sciences, SE-75007 Uppsala, Sweden
[b] College of Geography and Tourism, Hengyang Normal University, 421002 Hengyang, China
[c] Department of Forest Ecology and Management, Swedish University of Agricultural Sciences, SE-90183 Umeå, Sweden
[d] State Key Laboratory of Environmental Geochemistry, Institute of Geochemistry, Chinese Academy of Sciences, 550081 Guiyang, China
[e] Department of Marine Biology and Oceanography, Institut de Ciències del Mar (ICM-CSIC), Pg Marítim de la Barceloneta 37-49, E08003 Barcelona, Catalunya, Spain
[f] Department of Chemistry, Umeå University, SE-90187 Umeå, Sweden

Received 25 January 2021; accepted in revised form 4 June 2021; available online 12 June 2021

Abstract

A geographically constrained chronosequence of peatlands divided into three age classes (young, intermediate and old) was used to explore the role of biogeochemical influences, including electron donors and acceptors as well as chemical speciation of inorganic mercury (Hg(II)), on net formation of methylmercury (MeHg) as approximated by the fraction of MeHg to total mercury (THg) in the peat soil. We hypothesized that removing vascular plants would reduce availability of electron donors and thus net MeHg formation. However, we found no effect of the vascular plant removal. The sum of the potential electron donors (acetate, lactate, propionate and oxalate), the electron donation proxy organic C/Organic N, and the potential electron acceptors (Fe(III), Mn and sulfate) in porewater all showed significant correlations with the net MeHg formation proxies in peat soil (MeHg concentration and %MeHg of THg). Thus differences in both electron donor and acceptor availability may be contributing to the pattern of net MeHg formation along the chronosequence. In contrast, Hg(II) concentrations in peat porewater showed small differences along the gradient. A chemical speciation model successfully predicted the solubility of Hg and MeHg in the porewater. The modeling pointed to an enhanced concentration of Hg-polysulfide species in the younger peatlands as a potential factor behind increased Hg(II) solubility and methylation in the more nutrient-rich peatlands. This work contributes to the understanding of Hg and MeHg cycling in peatlands which can help guide mitigation measures to reduce aquatic MeHg biomagnification in peatland dominated landscapes.

Keywords: Mercury; Methylmercury; Chronosequence; Peatland; Porewater; Hg solubility; Chemical speciation

1. INTRODUCTION

Bioaccumulation of methylmercury (MeHg) is a major concern in northern aquatic ecosystems, especially those with peatlands in their catchments (Loseto et al., 2004; Macdonald et al., 2005; AMAP, 2011). MeHg in these

* Corresponding author at: College of Geography and Tourism, Hengyang Normal University, 421002 Hengyang, China.
E-mail address: zhongzsq@hynu.edu.cn (S. Zhong).

https://doi.org/10.1016/j.gca.2021.06.010
0016-7037/

systems mainly originates from biological methylation of inorganic mercury, Hg(II), a process that predominantly occurs under anoxic conditions (Compeau and Bartha, 1985; Benoit et al., 2003; Gilmour et al., 2013). Peatlands, which accumulate total mercury (THg) deposited from the atmosphere, are also sources of MeHg to downstream aquatic ecosystems (Mitchell et al., 2008b; St. Louis et al., 1996; Tjerngren et al., 2012b) and thereby contribute to MeHg bioaccumulation in fish. The consumption of these fish by humans and wildlife increases the risks for reaching harmful levels of Hg exposure in these higher trophic level consumers (Driscoll et al., 1994; Ratcliffe et al., 1996; Munthe et al., 2007). In addition to the direct hazards from Hg exposure, restrictions on the consumption of fish are in themselves a threat to human health and nutrition, since fish is an important source of proteins and contains fatty acids and other compounds that can benefit human health (Strandberg et al., 2016; Jing et al., 2020). Improved knowledge of the factors influencing net formation of MeHg in peatlands can thus advance the development of management strategies to more effectively mitigate the threat from Hg while promoting benefits from fish consumption.

The concentration of MeHg occurring in soils and waters is the net of Hg methylation (largely biotic) and MeHg demethylation reactions (which can be both biotic and abiotic) (Jensen and Jernelöv, 1969; Spangler et al., 1973). The former generally appears to be the more variable process (Drott et al., 2008; Tjerngren et al., 2012a; Hu et al., 2020), but changes in demethylation rates also contribute to differences in net MeHg formation (Kronberg et al., 2012). Manipulation experiments have emphasized the dependence of net MeHg formation on three categories of geochemical factors affecting biotic Hg methylation in the presence of suitable microbial communities: the availability of 1) electron donors (i.e. organic carbon with appropriate qualities) (Windham-Myers et al., 2009; Bravo et al., 2017; Zhu et al., 2018), 2) electron acceptors such as sulfate (Branfireun et al., 2001; Jeremiason et al., 2006; Mitchell et al., 2008a; Bergman et al., 2012) and 3) bioavailable Hg (Jonsson et al., 2014; Zhu et al., 2018). While there is a considerable body of research looking at these three factors, fewer studies look at all three factors together. Manipulation experiments also face challenges in generalizing to natural environments because of artefacts, such as unintended disturbance effects or the generally limited time periods for manipulations.

Exploration of the factors determined to influence net Hg methylation in manipulation experiments, such as sulfur and other nutrients, have been complemented by studies of peatlands along natural environmental gradients (Tjerngren et al., 2012a; Poulin et al., 2019; Åkerblom et al., 2020). A finding from such studies is that Hg methylation seems to increase along wetland trophic gradients that provide an increase in pH, nutrients and electron acceptor availability (particularly sulfate), as well as the nutrient demand of the plant community composition. The net MeHg formation appears to increase to a certain threshold, beyond which a further increase in the nutrient/trophic level of wetlands will result in a decreased net MeHg formation (Tjerngren et al., 2012a; Tjerngren et al., 2012b). Along many natural gradients though, independently varying differences in climate and management history complicate interpretations of causality.

Along the Baltic Sea's Bothnian Bay in northern Scandinavia, post-glacial land uplift has created a chronosequence of peatlands within the space of a few kilometers, all subjected to similar atmospheric deposition, underlying geology and climate patterns. Newly formed peat at the top of the soil profiles in these peatlands is progressively isolated from the underlying mineral substrates along a chronosequence from "younger" to "older" peatlands, creating gradients in peatland biogeochemistry (Tuittila et al., 2013). This means that with increasing age from a century to several millennia (defined by when peat development initiated), the concentrations of major mineral-derived elements (e.g. Ca, Mg, Fe and S) decline in the upper peat soil, resulting in a major change in vegetation and microbiological community composition along the chronosequence. This gradient provides an opportunity to investigate the effect of long-term biogeochemical influences, such as electron donors and acceptors, availability of Hg and nutrient status, on net MeHg formation without the need for long-term experimental manipulations.

In previous work influences of nutrients and other geochemical parameters on THg and MeHg concentrations in solid peat along a peatland chronosequence were investigated (Wang et al., 2020). The microbial metabolism (e.g. sulfate reduction, iron reduction, methanogenesis and fermentation) responsible for Hg methylation has also been studied in samples taken along the chronosequence (Hu et al., 2020). The inputs of root exudates from vascular plants have been shown to limit net MeHg production in salt marshes (Windham-Myers et al., 2009). Thus the removal of vascular plants can be used to test the hypothesis that net MeHg formation would decrease with declining availability of electron donors in vascular plant root exudates.

In this study, we use the concentration of MeHg and its fraction of total Hg (%MeHg) in the soil as proxies for net MeHg formation, which have been proven to be positively related to rates of net MeHg formation in experiments conducted in a range of different types of freshwater sediments (Drott et al., 2008). We go beyond previous work on a peatland chronosequence (Hu et al., 2020; Wang et al., 2020) to experimentally explore the influence of potential electron donors on net MeHg formation along the chronosequence by removing the vascular plants from the peatlands during two consecutive growing seasons. We also investigate how measured concentrations of potential electron acceptors in porewater, as well as the solubility of Hg and its chemical speciation co-varied with the net MeHg formation proxies along the chronosequence. Furthermore, geochemical modeling of Hg solubility and its chemical speciation facilitate a more thorough analysis of influences related to Hg bioavailability than has been possible before on this chronosequence and many other *in situ* studies of methylation in peatlands.

2. MATERIALS AND METHODS

2.1. Site description

A chronosequence of fifteen open boreal peatlands created by post-glacial land uplift along the Gulf of Bothnia was studied (Fig. 1a). Briefly, these fifteen peatlands are divided into three age classes, young (<1000 years, n = 5), intermediate (1000 ~ 2000 years, n = 5) and old (>2000 years, n = 5). The age of the peatlands was determined with the shoreline displacement curves developed from age determination based on varved lake sediment counting (Renberg and Segerström, 1981). The peatlands cover a natural gradient of trophic status and hydrogeochemistry. The older peatlands along this peatland chronosequence are more oligotrophic, indicated by decreasing pH, vascular plant cover and concentrations of major minerogenic elements (e.g. Fe, Ca, Mn, Mg, K,

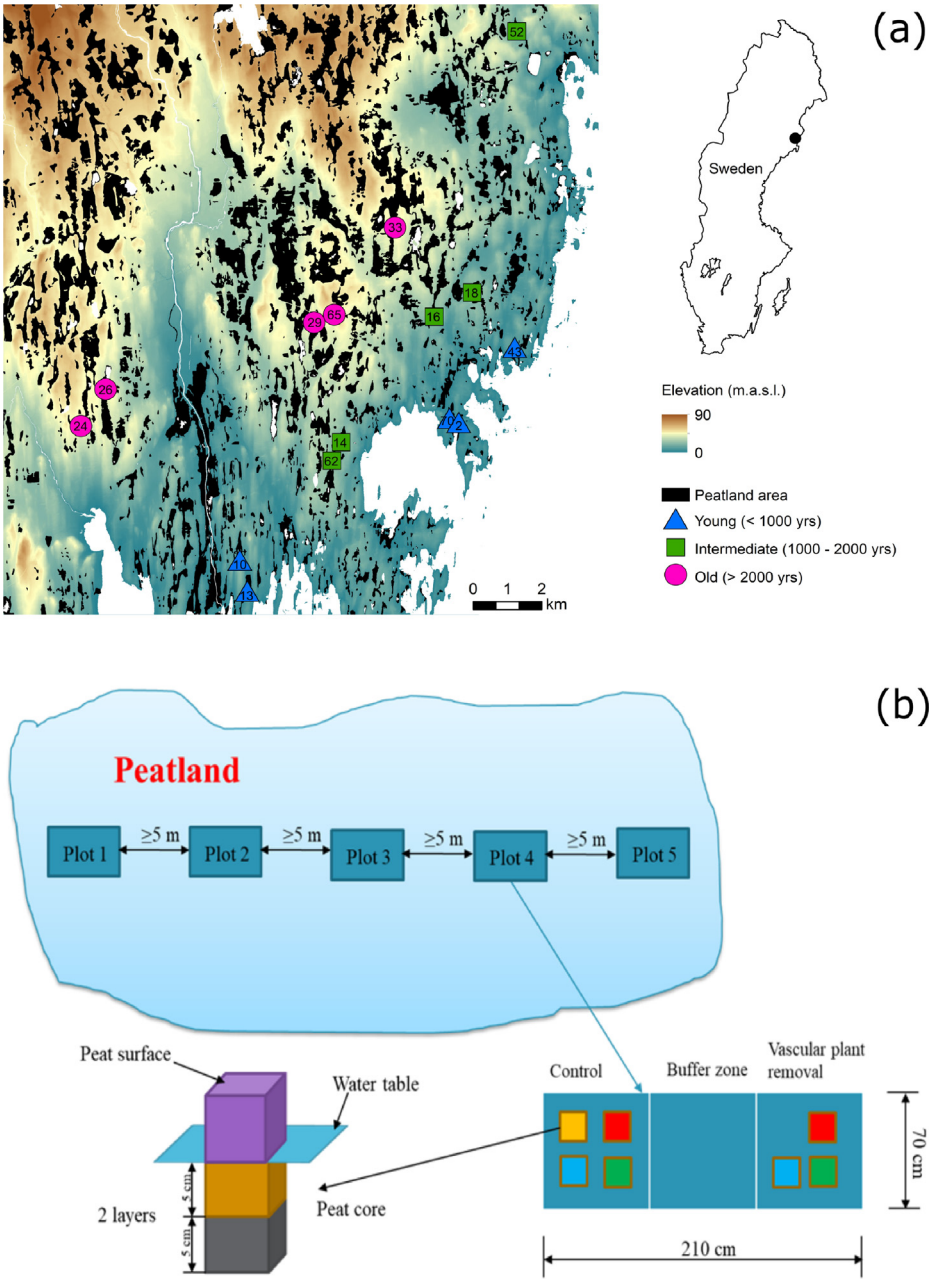

Fig. 1. (a) The fifteen peatland sites divided into three age classes along the chronosequence created by post-glacial uplift on the northeast coast of Sweden. (b) The five replicate experimental plots within each peatland site. Within each replicate plot there are control and vascular plant removal (VPR) subplots divided by a buffer. The four colored squares within each subplot represent the peat cores taken during the sampling campaigns in June and August of both 2016 and 2017. Since the vascular plants were removed for the first time in June 2016, the VPR subplots were only sampled three times, starting in August 2016. This figure is adapted from Wang et al. (2020).

Na) in superficial peat soil, as well as increasing total amount of carbon, peat depth and peatland area (Table S1 in the Supplementary information (SI)). Bulk density and C/N ratio of the peat did not differ significantly among the three peatland classes. This is, to some extent, an indication of similar peat decomposition rates. The field-layer plant community composition changes systematically with the peatland age and nutrient status. The vascular plants were dominated by forbs (e.g. *Epilobium palustre* and *Pedicularis palustris*) and tall sedges (e.g. *Carex rostrata* and *Carex limosa*) in the younger mesotrophic, minerogenic peatlands, while dwarf shrubs (*Andromeda polifolia* and *Vaccinium oxycoccus*) and low growing sedges (*Eriophorum vaginatum*, *Trichophorum spp*. and *Carex limosa*) were more common in the older and more oligotrophic peatlands. The intermediate peatlands were characterized by a vegetation transition between the young and old peatlands (Table S2). More details can be found in Wang et al. (2020) and Laine et al. (2021).

2.2. Vascular plant removal and sampling of peat soil and porewater

In June 2016, five 70 × 210 cm plots were established at least 5 m apart along a line across the center of each of the fifteen peatlands. Then each of the five 70 × 210 cm plots was divided into three 70 × 70 cm subplots: one subplot with all vascular plants removed and one control subplot as well as one buffer subplot between them (Fig. 1b). On the vascular plant removal (VPR) subplots, the biomass of all the vascular plants, forbs and shrubs, including their roots, was removed by hand, while mosses and lichens were left in the bottom layer. The VPR subplots were revisited to maintain the absence of vascular plants during the growing seasons of 2016 and 2017.

Peat soils were sampled from both control and VPR subplots on peat lawns according to the protocols of Wang et al. (2020). Data collected in August (growing season) 2016, June (beginning of growing season) 2017 and August 2017 were used in the current study, since these are the ones influenced by the removal of the vascular plants. Briefly, an individual cube-shaped core of peat soil (10 × 10 × 10 cm) was extracted immediately below the average growing season ground water table (GWT) from each control and VPR subplot within each peatland using a custom-made knife. The peat core was cut into upper and lower layers (0–5 and 5–10 cm below the GWT, respectively) that were sealed in separate zip-lock bags and kept cool and dark during transport to the lab. The peat samples from the same layers (upper or lower) and subplots (VPR or control subplot) of each peatland were homogenized into an individual sample with a 4 mm cutting sieve, after the removal of bulky roots, sticks and living plant material. The homogenized peat soil was then subsampled for chemical analyses including the total concentrations of elements (e.g. C, S and Fe) as well as concentrations of MeHg and THg.

Porewaters were sampled in June and August of 2017 from all the VPR and control subplots within each peatland. The porewater sampling employed the same method as described elsewhere (Branfireun et al., 2001; Liem-Nguyen et al., 2017). Briefly, porewater was sucked up into a 250 mL high-density polyethylene (HDPE) bottle from the specific soil depths where the corresponding peat core was extracted, using a custom-made probe consisting of a vacuum pump connected to a stiff Teflon tube where the last 10 cm were perforated and a pointed cap closed the end of the tube. Nitrogen gas was flushed through the tubing and sample bottle to keep the system deoxygenated during sampling. Porewater subsamples for the determination of sulfide and iron species were immediately collected from the HDPE bottle with a syringe, filtered through a 0.45 μm membrane filter in the field and then injected, through a rubber septum, into a pre-evacuated glass vial, leaving no headspace. In the glass vials for the determination of iron species, 15 μL of 2 M NaOH was added in advance. After porewater subsamples were taken for the determination of sulfide and iron species, the rest of the porewater in the HDPE bottle was discarded and the bottle was refilled without headspace. All the porewater samples in HDPE bottles or glass vials were kept dark and cool during transport to the lab and stored in a refrigerator at 4 °C until further processing. The next day, the five HDPE bottles with porewater samples from the same subplots (VPR or control) were filtered through a funnel filter (Restek) with a pore size of 0.22 μm using a vacuum pump in a glovebox with nitrogen gas atmosphere. A 50 mL aliquot of porewater was taken from each of the five filtered porewater samples and mixed into a 250 mL bulk sample for that subplot. Porewater subsamples were then collected from the homogenized bulk sample for porewater chemical analyses such as dissolved organic carbon (DOC) and concentrations of major ions.

2.3. Chemical analyses

In the peat soil samples, total concentrations of elements such as C, N, S, P, Mn, Mg and Fe, as well as concentrations of total Hg and MeHg were determined according to Wang et al. (2020). In porewater, pH was determined in the filtered porewaters in 2017, while in 2016 the pH was determined in the field in porewater that immediately refilled the sample hole. The dissolved organic carbon (DOC) and nitrogen (DON) were measured with a Shimadzu analyzer (TOC-VCPH and TNM-1 units for DOC and DON, respectively; Shimadzu, Japan). The porewater absorbance of light at 254 nm (/cm), subtracted by the light absorbance of Fe (calculated as, Fe_{254nm} (/cm) = 0.085 × [Fe_{TOT}] (mg/L) + 0.0007, Weishaar et al. (2003)), was divided by DOC (mg/L) and multiplied by 100 to yield the specific UV absorbance (SUVA, L/mg(C)/m). Concentrations of total dissolved inorganic sulfide, S(−II), were determined by the method of Cline (1969), after sample preservation with ZnAc (Liem-Nguyen et al., 2017). Concentrations of major anions (e.g. Cl^- and SO_4^{2-}) and low molecular mass organic acids (LMM OA:s) (i.e. acetate, lactate, propionate, oxalate) were quantified on a Metrohm IC system (883 Basic IC Plus and 919 Autosampler Plus) with detailed analytical information listed in Table S3. Concentrations of major cations (e.g. Na, K, Ca, Mg,

Mn, Al, Fe) were determined by inductively coupled plasma atomic emission spectroscopy. Concentrations of Fe(II) and Fe(III) were determined by UV absorption spectrophotometry according to the method of Viollier et al. (2000). Concentrations of THg in porewaters were measured by isotope dilution analysis (IDA) using mercury cold vapor generation coupled to inductively coupled plasma mass spectrometry after digestion with BrCl. Concentrations of MeHg in porewater were conducted by IDA using purge and trap thermal desorption coupled to gas chromatography ICP-MS (Lambertsson and Björn, 2004). Concentrations of inorganic Hg(II) in soils and porewaters were calculated by subtracting MeHg from THg. The percentage of MeHg to THg (% MeHg) in peat soil was calculated as a proxy for net MeHg formation (Drott et al., 2008). The certified reference materials MESS-3 (0.091 ± 0.009 mg Hg/kg) and ERM-CC580 (0.075 ± 0.004 mg MeHg/kg) were used for quality control of the THg and MeHg in soil measurements, respectively. Replicate samples and reference materials were analyzed regularly for all the measurements in this study and the accuracy (defined as measured divided by certified concentrations) was 95 ± 5 and 105 ± 8% for MESS-3 and ERM-CC580, respectively while the precision was better than 10% relative standard deviation. The detection limits for concentrations of MeHg and THg in porewater were ~ 0.004 and 0.06 ng/L, respectively.

2.4. Chemical speciation modeling

The chemical speciation modeling of Hg(II) and MeHg in the peatland soils and porewaters along this peatland chronosequence was built on the model of Liem-Nguyen et al. (2017) applied to data collected in four different types of wetland soils, and was refined by adjusting the log K for the formation of HgS(s) to either of the two experimentally determined constants reported by Drott et al. (2013) and Schwarzenbach and Widmer (1963).

Briefly, thermodynamic calculations were made in the Microsoft Excel program using an iterative procedure where either the adsorbed/solid (ads) phases Hg $(NOM-RS)_2$ (ads) or metacinnabar, β-HgS(s), were in control of the aqueous concentration of the Hg^{2+} ion, which in turn was a component in all chemical reactions. Input data were soil water contents and total soil concentrations of Hg (II), MeHg, sulfur (S_{TOT}), and organic carbon (C_{TOT}), concentrations of thiol groups associated to NOM (NOM−RSH, including adsorbed/solid and aqueous (aq) phases: NOM−RSH(ads) and NOM−RSH(aq), respectively) and aqueous phase concentrations of DOC, Cl^-, HS^-, Fe(II) as well as pH (Table S4). The chemical reactions and their thermodynamic constants used in the modeling are listed in Table S5. The solubility of Hg(II) and MeHg was determined as the solid-solution partition coefficient, $\log K_{d\ (Hg)} = \log([\text{peat Hg}]/[\text{porewater Hg}])$ (L/Kg) and $\log K_{d\ (MeHg)} = \log([\text{peat MeHg}]/[\text{porewater MeHg}])$ (L/Kg). The model fit (merit-of-fit) was evaluated by comparing modeled and measured data on log K_d and absolute concentrations of Hg and MeHg calculated by the following equation: merit-of-fit $R_P\% = \Sigma(\text{data}_{\text{modeled}} - \text{data}_{\text{measured}})^2/\Sigma\text{data}^2_{\text{measured}}$.

While most of these input data were measured in the porewater and soil, the concentration of NOM−RS_{TOT} (the sum of protonated, dissociated and metal complexed NOM-RS functionalities) was calculated based on measurements from the study of Liem-Nguyen et al. (2017). They used Hg L_{III}-edge extended X-ray absorption fine structure spectroscopy (EXAFS) to determine the concentration of NOM−RS_{TOT}. The concentration corresponded to 15% of the reduced organic S (Org-S_{RED}) in the peat soils at site "SKM", a site that can be considered representative for the "old peatlands" in the chronosequence (it was taken from the same region from a peatland having similar age, biogeochemistry and trophic status as our old peatlands). At this site, Org-S_{RED} comprised 65% of S_{TOT} as determined by sulfur K-edge X-ray absorption near-edge structure (XANES) spectroscopy. Thus, the total concentration of NOM−RS_{TOT} in percentage of S_{TOT} is calculated as $0.15 \times 0.65 \times 100 = 9.8\%$. Even though this value is expected to reflect the old peatlands better than the young and intermediate peatlands, we used this value of 9.8% of S_{TOT} as an estimate of the concentration of NOM−RS_{TOT}(ads) in all peat soils along the chronosequence. The concentration of NOM−RS_{TOT}(aq) in specific samples was calculated from the DOC/SOC ratio, assuming the same concentration of NOM−RS_{TOT} functional groups per organic C in aqueous and solid/adsorbed phases of the peat.

Elemental S was present in all peatland soils of the study by Liem-Nguyen et al. (2017), including soils having similar properties as the old peatlands in this study. Therefore, Hg-polysulfide formation was considered in our model, by including the HgS_nHS^- and $Hg(S_n)_2^{2-}$ species (Skyllberg, 2012). Notably, complexes with Cl^- (<0.8 mM) did not contribute significantly to the solubility of Hg(II) in the porewaters of the chronosequence peatlands. Ionic strength effects were also low (I < 1.5 mM in all samples) and considered negligible in relation to uncertainties in thermodynamic constants. Thus, no ionic strength corrections were made for constants used in the calculations (I = 0 M). The possible presence of the mineral mackinawite (FeS_m) in the peatlands was examined by calculation of the ion activity product ($IAP = [Fe^{2+}][HS^-]/[H^+]$) for the reaction: $FeS_m + H^+ = Fe^{2+} + HS^-$. The HS^- concentrations were recalculated from S(−II) using a pK_a of 7.0 for H_2S(aq) (Millero et al., 1988).

2.5. Statistics

All the data were tested for normality and homogeneity prior to statistical analyses using the Shapiro-Wilk and Levene tests, respectively. Log transformation was applied when the original data were not normally distributed. A non-parametric Kruskal-Wallis test was conducted for non-normally distributed data even after log transformation and followed by a pairwise Wilcoxon rank sum test if there was any significant difference. Significant differences in geochemical parameters in both peat soil and porewater between

the three peatland age classes (young, intermediate and old peatlands) were tested for using univariate Analyses of Variance (ANOVA), followed by Tukey's multiple comparison test. The effects of vascular plant removal were tested by two-way ANOVA, followed by Tukey's multiple comparison test. As the porewater sampler is 10 cm in length, the average values were applied for peat soil geochemical parameters in both 0–5 and 5–10 cm layers corresponding to the 10 cm profile where the porewater was sampled, when testing for the effects of vascular plant removal and the relationships between the geochemical parameters in peat soil and in porewater. Pearson correlations were applied to test relationships between geochemical parameters. All the statistical tests in this study were carried out using R program (Version 3.6.3) at the significance level of 0.05.

3. RESULTS

3.1. Differences in MeHg, Hg(II) and general geochemical parameters along the peatland chronosequence

There was a significant difference in Hg(II) concentrations in peat soil along the chronosequence, with the lowest concentrations in the young and highest concentrations in the older peatlands, while porewater concentrations did not differ among the three peatland age classes (Fig. 2, Table S1, Table S6). Peatlands of young and intermediate age had significantly higher concentrations of MeHg and %MeHg in both peat soil and porewater as compared to old peatlands (Fig. 2, Table S1, Table S6, Table S7). When it comes to the general geochemistry, there was significantly lower pH, as well as lower concentrations of some of the major metal cations (Ca, Mg, K, Fe) in the old peatlands as compared to the other two age classes. This reflects the gradual isolation of the top peat layers from the underlying mineral soils with increasing age of the peatlands, resulting in higher acidity and more oligotrophic conditions at the older end of the chronosequence (Fig. 3, Table S6).

3.2. The importance of potential electron donors on net MeHg formation

3.2.1. Effects of removing vascular plants along the peatland chronosequence

Our hypothesis was that the VPR would reduce inputs of high-quality organic carbon sources (i.e. root exudates) for Hg methylating microorganisms in the rhizosphere and subsequently reduce microbial net MeHg formation. However, there were no differences in net MeHg formation proxies (MeHg concentration and %MeHg) in solid peat or porewater between the control subplots and those where the vascular plants had been removed in young, intermediate or old peatlands (Fig. 2, Table S6, Table S7). The VPR also did not create any detectable changes in major biogeochemical parameters in either peat soil (e.g. C/N, element concentrations; Table S1) or porewater (e.g. pH, DOC, anion or metal cation concentrations, or LMM OA:s; Fig. 4, Table S6). Samples collected from the VPR subplots were therefore treated as replicates of control samples for subsequent data analyses.

3.2.2. Differences in potential electron donors along the chronosequence and correlations with net MeHg formation proxies

The concentration of LMM OA:s in the porewater differed significantly among the three age classes of peatlands, with the youngest peatlands showing the highest concentrations of the sum of all LMM OA:s, as well as of the individual components acetate, lactate and propionate (Fig. 3d, Fig. 4, Table S6). Neither the DOC concentration (26.4 ~ 100.0 mg/L) nor its aromatic character, as indicated by SUVA, showed any significant differences among the three peatland age classes (Fig. 3b, f, Table S6). The sum of LMM OA:s also demonstrated a positive, significant relationship with the net MeHg formation proxies MeHg and %MeHg in peat soil (Fig. 5a, b), with the exception for MeHg in peat soil (Fig. 5a). A positive relationship was also observed with the same parameters in the porewater (Fig. S1a, b).

The DOC/DON ratio in the porewater showed significant differences between the young (55 ± 14 g/g, mean ± standard deviation) and old (77 ± 11 g/g) peatlands (Fig. 3e). In the population of all data, the DOC/DON ratio was significantly, negatively correlated with MeHg and %MeHg in peat soil (Fig. 5c, d) and porewaters (Fig. S1c, d), with the exception for MeHg in peat soil (Fig. 5c; $p = 0.11$). The DOC did not show any significant correlation with net MeHg formation proxies (data not shown), while SUVA was significantly, positively correlated with %MeHg in peat soil ($p < 0.001$, $r = 0.42$) and with MeHg in porewater ($p = 0.04$, $r = 0.27$).

3.3. Differences in concentrations of potential electron acceptors along the chronosequence and correlations with net MeHg formation proxies

Although porewater sulfate concentrations (0.3 ~ 2.5 mg/L) did not differ significantly among the three peatland age classes (Fig. 3i, Table S6), there were significant and positive correlations between sulfate concentrations and MeHg as well as %MeHg in both peat soil (Fig. 6a, b) and porewater (Fig. S2a, b), with the exception that sulfate concentrations did not correlate significantly to %MeHg in peat soil (Fig. 6b). Inorganic S(−II), the result of dissimilatory sulfate reduction, was present in the porewaters of all the peatlands, but the concentrations (0.3 ~ 1.2 μmol/L) were in many cases close to the detection limit of 0.2 μmol/L and did not differ between the three peatland age classes (Fig. 3c, Table S6). Porewater concentrations of S(−II) were not significantly correlated with either concentrations of sulfate (n = 30), MeHg (n = 60) or % MeHg (n = 60) in porewater. Porewater S(−II) was not correlated with MeHg concentration in solid peat, but it correlated negatively with %MeHg in soil (n = 60, $r = -0.27$, $p = 0.04$).

Porewater concentrations of Fe(III) (0.5 ~ 47.1 μmol/L) were significantly higher in young peatlands compared to old peatlands (Fig. 3h, Table S6) and positively correlated with MeHg and %MeHg in both peat soil (Fig. 6c, d) and porewater (Fig. S2c, d) across the peatland chronosequence. Ferrous iron, Fe(II), (0.7 ~ 95.1 μmol/L), the pro-

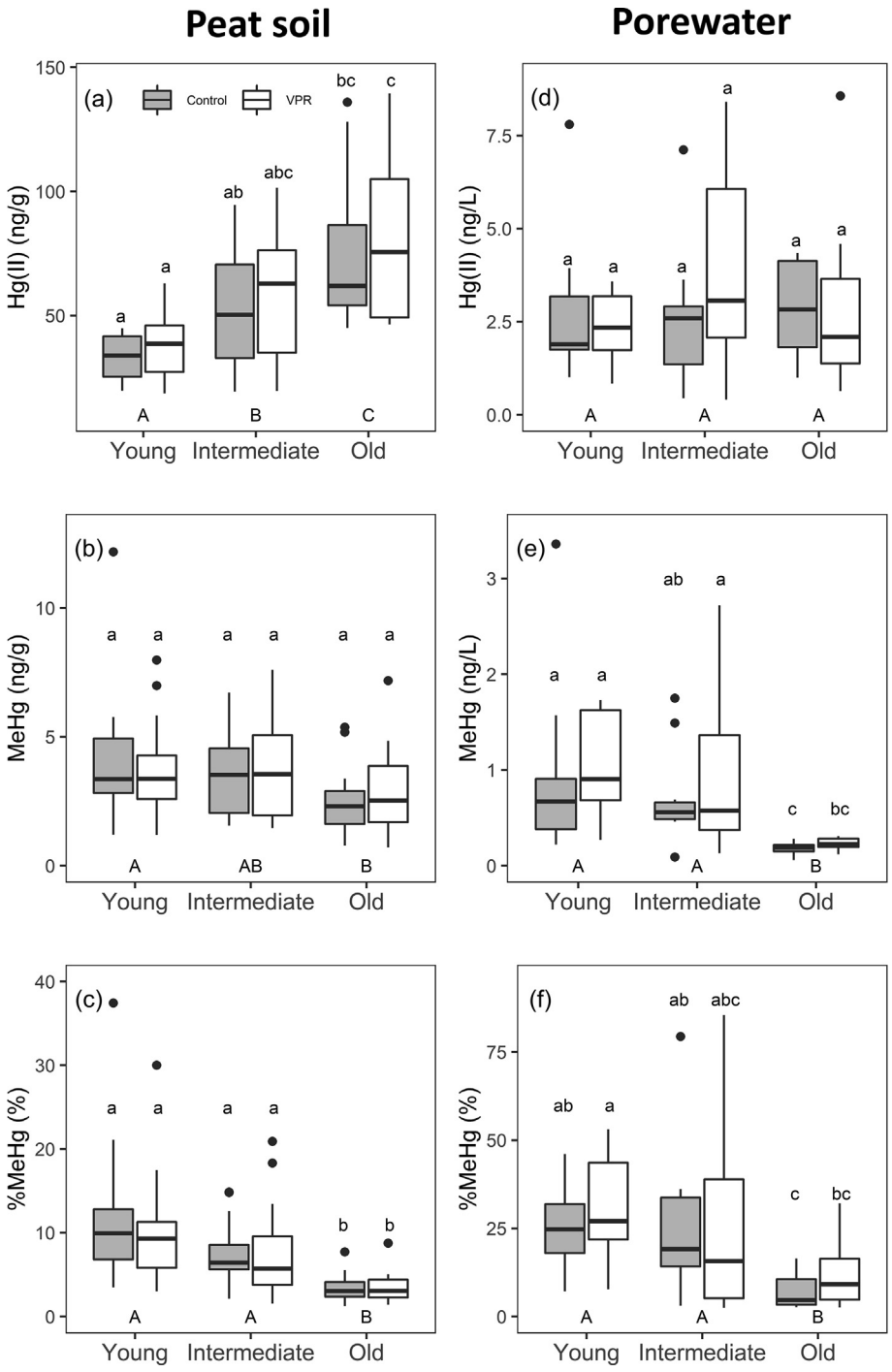

Fig. 2. Effects of vascular plant removal (VPR) on (a, d) Hg(II), (b, e) MeHg concentrations and (c, f) %MeHg in peat soil (left panel) and porewater (right panel) in the three age classes of peatlands along the chronosequence. Concentrations of MeHg and %MeHg in peat soil are average values of 0–5 and 5–10 cm layers at the three sampling occasions in 2016 and 2017 (n = 90). Concentrations of MeHg and %MeHg in porewaters are for 0–10 cm layers sampled in 2017 (n = 60). Different lowercase letters above the boxes indicate significant differences between control and VPR subplots. Different uppercase letters below the boxes indicate significant differences between the three peatland age classes. The same letters indicate no significant difference.

duct of dissimilatory Fe(III) reduction, was predominant in porewaters of most peatlands studied and exhibited a positive correlation with Fe(III) concentrations (Fig. S3, Table S6) as well as with MeHg concentrations and % MeHg in peat soil and porewater along the peatland chronosequence.

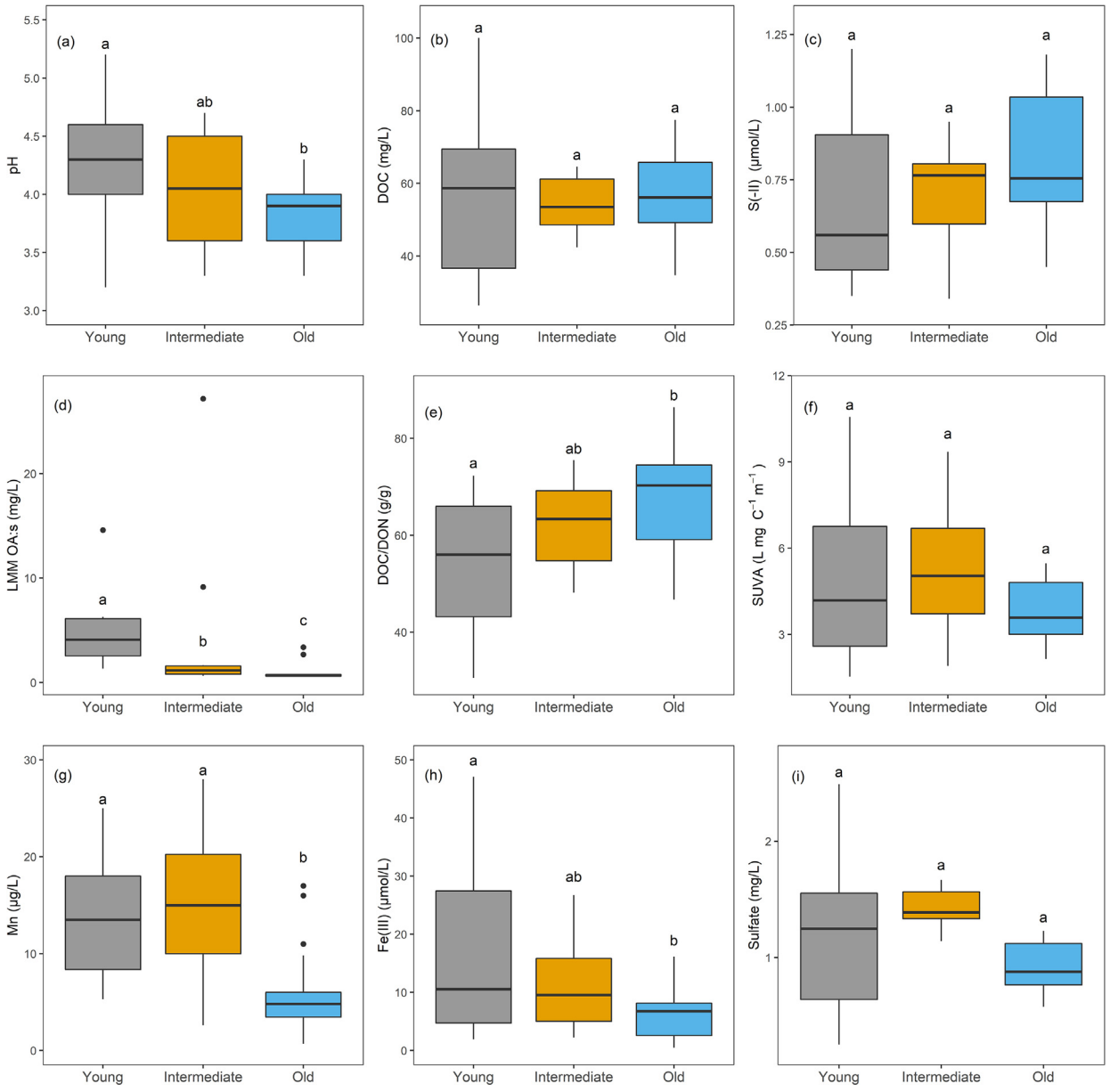

Fig. 3. Porewater chemistry in peatlands of the three age classes along the chronosequence. Because removing the vascular plants had no significant effect on the geochemistry (Table S7), the values from subplots with and without vascular plants are grouped together by age class for each of the two sampling occasions in 2017. Different letters above the boxes indicate significant differences between the three peatland age classes. Boxes with the same letters indicate no significant difference.

The mineral FeS_m (mackinawite) did not appear to be present in any of our soil samples, even though it is formed by a reaction between HS^- and Fe(II) ions. The calculated log IAP averaged −10.1, −10.6 and −11.5 in young, intermediate and old peatlands, respectively (Table S4). These values are all much lower than the theoretical value in the presence of FeS_m of −3.5, which indicates that the porewater was highly undersaturated relative to what would be expected if the mineral were present (Rickard, 2006).

3.4. Solubility and chemical speciation of mercury and methylmercury

The aqueous phase concentration and chemical speciation of Hg(II) and MeHg is a factor that is known to be of importance for net MeHg formation and the uptake of MeHg in aquatic organisms, respectively. Although the Hg(II) concentrations in the peat soils decreased significantly along the chronosequence (old > intermediate > young), the concentration of Hg(II)

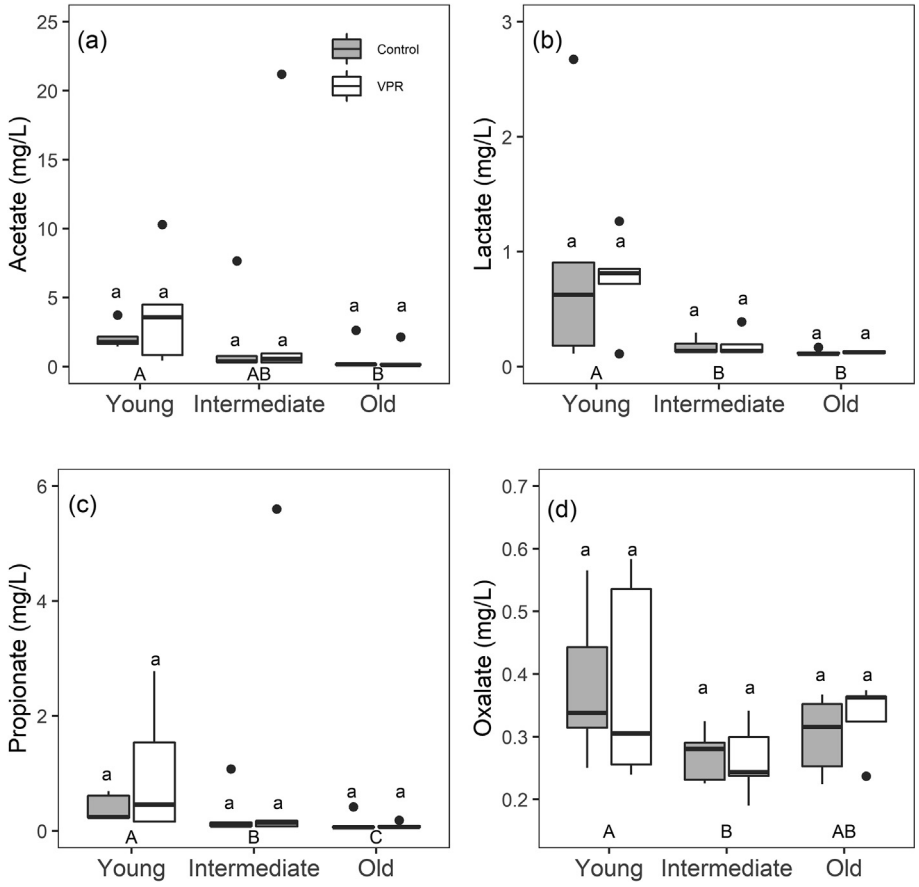

Fig. 4. Effects of vascular plant removal (VPR) on the formation of (a) acetate, (b) lactate, (c) propionate, and (d) oxalate in peatlands of the three age classes along the chronosequence. The lowercase letters above the boxes indicate significant differences ($p < 0.05$) between control and vascular plant removal plots of each age class. The uppercase letters below the boxes indicate significant differences between the three peatland age classes. The same letters indicate no significant difference (n = 30).

in porewater did not differ (Fig. 2). There were also no significant correlations between porewater Hg(II) concentrations and the net MeHg formation proxies (MeHg and % MeHg) in either solid peat (Fig. S4a, b) or porewater (data not shown). To further investigate if the chemical speciation of Hg in porewater differed among the age classes of peatlands, we applied a thermodynamic model.

In a first approach we applied a pure organic model in which the formation of both HgS(s) and Hg-polysulfide were excluded. This very simple model A worked out slightly better for the old peatlands (data more centered around the 1:1 line) than for the young and intermediate peatlands (Fig. 7a, b). The overall model fit was however greatly improved by the inclusion of HgS(s) and Hg-polysulfide formation (Table S8), with the best merit-of-fit of 0.10 obtained for model E, having a log K value of 36.8 for the formation of HgS(s) (Table S8, Fig. 7c, d). This value was experimentally determined for a crystalline form of metacinnabar, β-HgS(s), by Drott et al. (2013). Interestingly, also in the study of Liem-Nguyen et al. (2017) this log K value provided the best fit to data in organic soils with S (−II) concentrations less than 1 μM, very similar to most of the samples in our study. Overall, the model showed a generally better fit to the old peatland data, with a tendency to underestimate the solubility in young and intermediate peatlands (data points above the 1:1 line in Fig. 7c and below the line in Fig. 7d).

The solubility of MeHg was higher in the young and intermediate peatlands than in the old peatlands (i.e. lower log K_d MeHg; Table S4). When modeling the solubility and chemical speciation of MeHg, the log K value of 17.5 used for the reaction $MeHg^+ + NOMRS^- = MeHgNOM{-}RS$ (aq, ads) by Liem-Nguyen et al. (2017) resulted in a reasonably good fit for aqueous MeHg concentrations (Fig. S5a). An adjustment of the constant to a lower value improved the model fit for the solubility of MeHg (i.e. the log K_d), but not for the aqueous MeHg concentrations (data not shown). Similar to Hg(II), the solubility of MeHg in the young and intermediate peatlands was underestimated by the chemical speciation modeling, while the solubility of MeHg in the old peatlands was slightly overestimated (Fig. S5b).

4. DISCUSSION

4.1. General trends in net MeHg formation along the chronosequence

With peatland age along the chronosequence, there was a clear decrease in the net MeHg formation proxies (MeHg

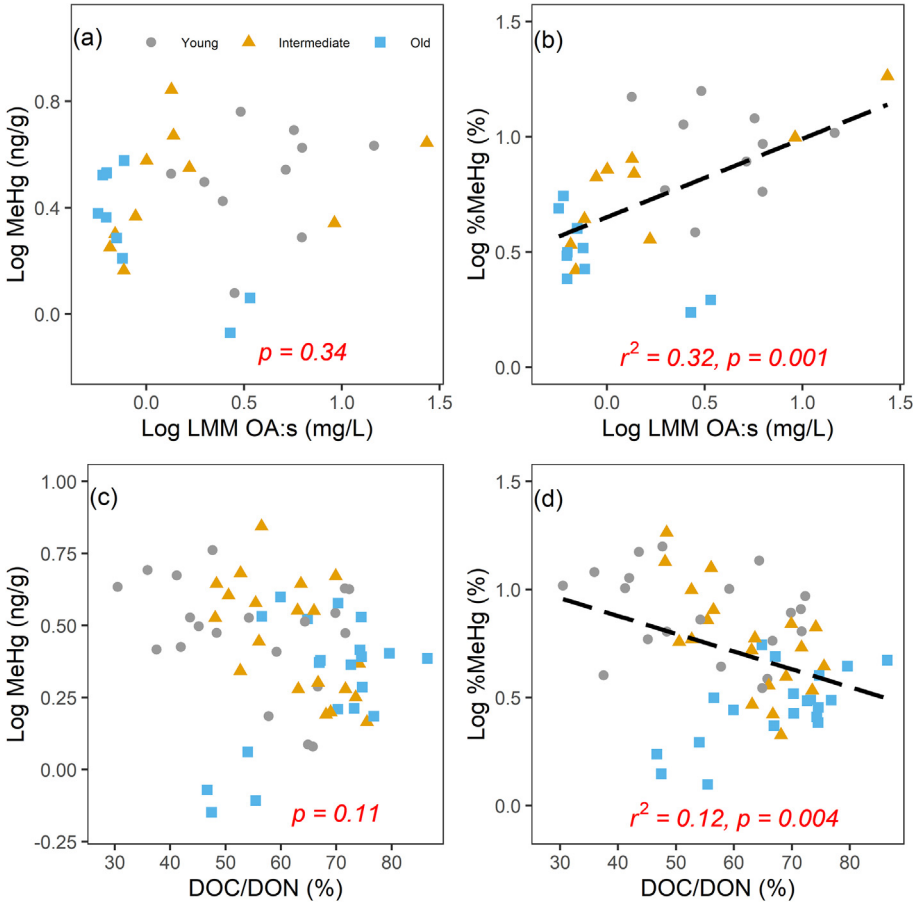

Fig. 5. Relationships between proxies for net MeHg formation (MeHg and % MeHg in peat soil) and (a, b) porewater concentrations of potential electron donors: total LMM OA:s (n = 30) as well as (c, d) the proxy for electron donors: DOC/DON ratio (n = 60).

and %MeHg) in peat, as well as the same measures in porewater (Fig. 2). Similar findings were reported for MeHg and %MeHg based on peat soils from this chronosequence (Wang et al., 2020), and the current study incorporates those data. This pattern of increased net MeHg formation from old to young peatlands along the chronosequence was further corroborated by experimentally determined rates of Hg(II) methylation (k_m) and demethylation (k_d), as well as their ratio (k_m/k_d), in soils along the same gradient (Hu et al., 2020). Because the age classes reflect a trophic and nutrient gradient (Fig. 3, Table S1) with the older peatlands being more oligotrophic/ombrotrophic (having deeper peat layers, lower pH, less vascular plant cover and lower concentrations of major minerogenic elements), the net MeHg formation clearly increases with increased nutrient availability and trophic level (Hu et al., 2020; Wang et al., 2020). Thus, we can conclude that both short-term (24 h) experimental determinations (k_m/k_d ratio) and the longer-term proxy (%MeHg in peat) demonstrate a clear increase in net MeHg formation with increasing nutrient and trophic status of the peatlands along the chronosequence.

Similar positive relationships between nutrient/trophic status and net MeHg formation proxies have been observed in other boreal peatlands (Tjerngren et al., 2012b; Gordon et al., 2016; Poulin et al., 2019). It should be noted that the range of peatlands studied here represents the nutrient-poor half of the conceptual model for MeHg net production as a function of trophic status, launched by Tjerngren et al. (2012a; 2012b). Thus, considering the biogeochemical properties and %MeHg in the peat, the young peatlands in the present study would correspond to peatlands with an intermediate trophic level having a relatively high methylation to demethylation ratio, as illustrated in Fig. S6 (Tjerngren et al., 2012a; Tjerngren et al., 2012b).

4.2. The vascular plant removal experiment

Vascular plants are a major driver of microbial community composition in peatlands through the labile C released as root exudates (Bragazza et al., 2015). However, the lack of any effect from VPR on either of the two net MeHg formation proxies MeHg and %MeHg in solid peat, or on the same parameters measured in porewater in this study (Fig. 2, Table S7), is different from other reports where the removal of plants decreased net MeHg formation in wetlands (Windham-Myers et al., 2009). Nevertheless, in a study of tidal freshwater wetlands, there was no

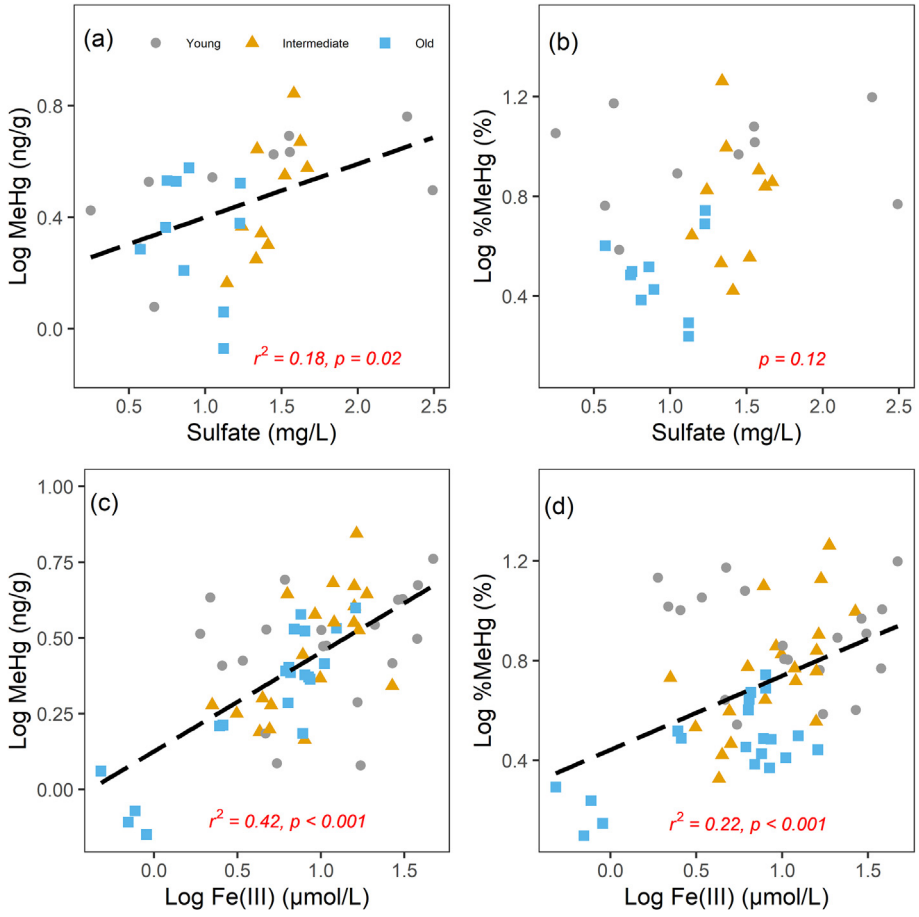

Fig. 6. Relationships between proxies for net MeHg formation (MeHg and % MeHg in peat soil) and potential electron acceptors in porewater: (a, b) sulfate (n = 30) and (c, d) Fe(III) (n = 60).

discernible effect of plant removal on methanogenesis (Keller et al., 2013), a key metabolic process of potentially high importance for Hg methylation (Hamelin et al., 2011).

So why did our VPR experiment not affect net MeHg formation as we had hypothesized? One obvious explanation would be that the VPR did not change the concentration of potential electron donors. Indeed, there were no significant differences in the porewater concentrations of any single LMM OA (acetate, lactate, propionate and oxalate, Fig. 4), or consequently the sum of LMM OA:s (data not shown), between the control and VPR subplots in any of the three age classes. Notably, there were also no detectable changes in any of the other measured parameters either, such as MeHg, Hg(II), other major element concentrations in peat soil, DOC or major ion concentrations in porewater (Fig. 2, Table S1, Table S6). Thus, from our VPR experiment it may be concluded that processes besides plant C exudation *per se* during the two-year study period are controlling concentrations (and possibly fluxes) of LMM OA:s in these peatlands. Those other processes could include microbial metabolism and degradation of organic matter. Of course, degradation of vascular plant biomass would still be expected to serve as a substrate for microorganisms responsible for organic matter degradation processes in these types of peatlands dominated by less degradable organic matter from Sphagnum mosses.

4.3. The potential impact of electron donors and acceptors on net MeHg proxies along the chronosequence

It is well-established that LMM OA:s and labile organic matter provide energy substrate for syntrophic microbial interactions between Hg methylating methanogens and SRB (Liu and Conrad, 2017; Yu et al., 2018). Even though there were no significant differences in the porewater concentrations of LMM OA:s between the control and VPR subplots, the concentrations of acetate, lactate, propionate and oxalate, as well as the sum of LMM OA:s were significantly higher in the younger peatlands (Fig. 3, Fig. 4). The electron-donor proxy DOC/DON (inversely related to the lability of DOM for microbial degradation) was also significantly lower in the young peatlands, as compared to the old peatlands (Fig. 3e; Table S6). This suggests that electron donation is an important factor behind the patterns in net MeHg formation proxies MeHg and %MeHg observed along the peatland chronosequence. In line with this, the data from all sites plotted together revealed significant relationships between both net MeHg formation prox-

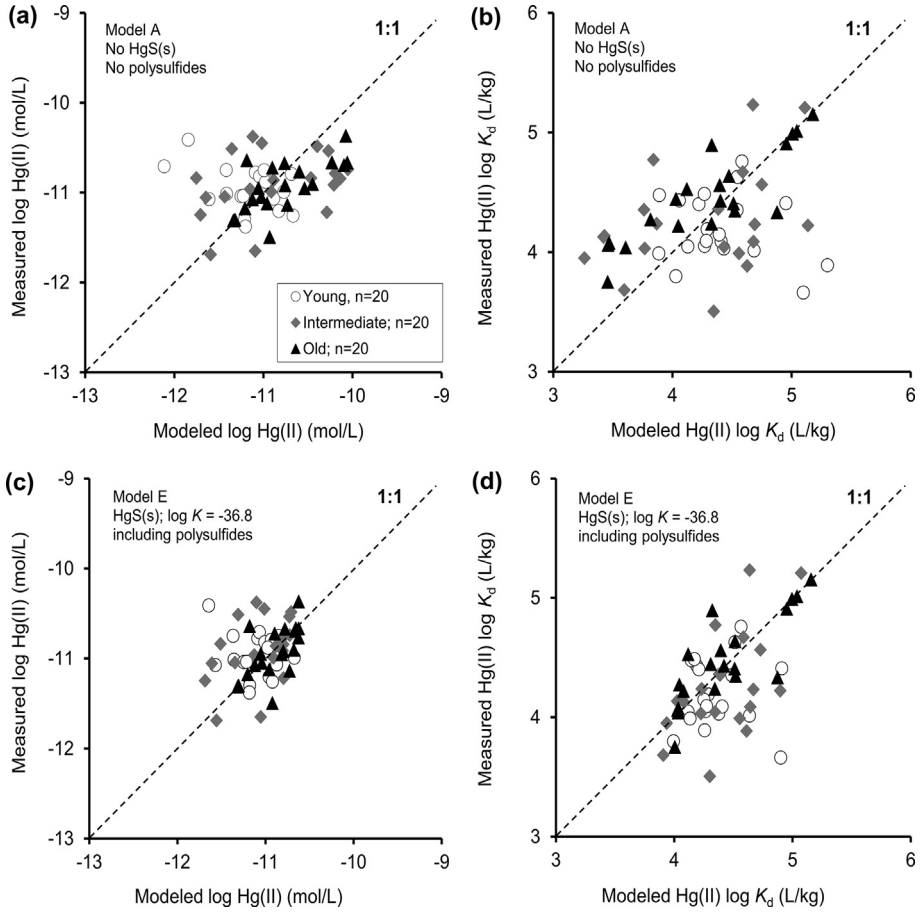

Fig. 7. Evaluation of a thermodynamic model for Hg(II) solubility in porewater along the peatland chronosequence without (a, b) and with (c, d) inclusion of HgS(s) and polysulfide formation. The left panels (a, c) are for log aqueous phase concentrations of Hg(II) and the right panels (b, d) are the corresponding data for log K_d.

ies and LMM OA:s as well as the DOC/DON ratio, respectively (Fig. 5).

There were generally higher concentrations of potential electron acceptors (e.g. Fe and Mn) in the younger peatlands along this chronosequence, although the concentration of sulfate did not show any significant difference among the age classes (Fig. 3). Moreover, The parallel patterns of Fe(III) and Mn, and to some extent sulfate, covaried positively with net MeHg formation proxies MeHg and %MeHg in peat soil as well as the same measures in porewater (Fig. 6, Fig. S2). All these results suggest that these potential electron acceptors may be of importance for the differences observed in the net MeHg formation along the peatland gradient. The relationship with Mn may indicate Mn reducing microorganisms are involved in net MeHg formation but also abiotic reduction of Mn oxides by Fe(II) (Villinski et al., 2001) may explain the similar patterns of Fe(III) and Mn (Fig. 3).

The positive relationship observed between sulfate and MeHg concentration in peat along the peatland chronosequence in the present study is in agreement with the reports from other wetland gradients (Mitchell et al., 2008b; Tjerngren et al., 2012a; Li et al., 2019; Åkerblom et al., 2020), where sulfate has been suggested to limit Hg methylation across wide gradients in sulfate supply. This is in agreement with a theoretical model by Langer et al. (2001). However, negative relationships between sulfate and MeHg net formation proxies can also be expected if studies are restricted to areas having similar supplies of sulfate and the activity of anaerobic microorganisms depleting sulfate to produce sulfide in the process of MeHg formation (Gilmour et al., 1998; Mitchell et al., 2008b; Skyllberg et al., 2009; Hoggarth et al., 2015; Li et al., 2019). The same can hold true for negative relationships between net MeHg formation proxies and Fe(III), and positive relationships with Fe(II), if the activity of iron-reducing bacteria parallels net MeHg formation (Skyllberg et al., 2009; Si et al., 2015).

It is interesting to note that in short-term (24 h) incubation experiments conducted with peat soils taken from the young, intermediate and old peatlands along this chronosequence, neither additions of the potential electron donors (LMM OA:s lactate + propionate + butyrate) nor additions of the potential electron acceptors sulfate or Fe(III) had stimulatory effects on the rates of MeHg formation (Hu et al., 2020). In these experiments it was demonstrated that SRB dominated MeHg formation in the young peatlands and methanogens and syntrophs involving SRB were more important in the older peatlands. Thus, for both

electron donors and acceptors, no short-term limitation of MeHg formation was discovered in the soil incubation experiments. Nonetheless, both types of components differed significantly in their porewater concentrations along the peatland chronosequence and showed positive correlations with the net MeHg formation proxies MeHg and % MeHg in the peat. This could be explained by the dual impacts of specific electron donors/acceptors on both the composition and activity of the peatland microbial community. This means that the changes in composition and amounts of electron donors/acceptors along this peatland chronosequence can have long term effects on the microbial structure and function and consequently net MeHg formation.

4.4. the potential influences of Hg solubility and chemical speciation on net MeHg formation proxies

Our previous work along the chronosequence and several other studies along natural and experimental gradients in Swedish peatlands have reported a negative relation between MeHg and THg concentrations in solid phase peat (Åkerblom et al., 2013; Wang et al., 2020). In this study, there was no difference in porewater Hg(II) concentrations between the three peatland age classes along the chronosequence (Fig. 2b, Table S6), even though the older peatlands had higher Hg(II) concentrations in the solid peat (Fig. 2a, Table S1). Also, concentrations of Hg(II) in porewater were not correlated with either MeHg or %MeHg in the peat soil (Fig. S4a, b). This suggests that Hg(II) concentrations, whether in the soil or its porewater, were not limiting net MeHg formation along the gradient.

It is, however, the bioavailable fraction of Hg(II), and not the total porewater Hg pool, that is expected to be of importance for bacterial uptake and thus for Hg methylation (Jonsson et al., 2014; Zhu et al., 2018). Studies have suggested that the complexation of Hg(II) by sulfide and polysulfides may alter the bioavailability of Hg(II) (Benoit et al., 1999; Ravichandran et al., 1999; Jay et al., 2000; Graham et al., 2017).

Thermodynamic modeling of the chemical speciation indicated that Hg(II) had slightly higher solubility in young peatlands ($p = 0.07$; which was also observed in measurements, Table S4) and that Hg-polysulfides were of importance for the overall Hg(II) solubility (Fig. 7, Table S8). This modeling result is explained by the relatively higher pH in the young peatlands, which facilitates the formation of polysulfides that complex with Hg(II), increasing the solubility of HgS(s) and possibly the bioavailability for methylating microorganisms (Jay et al., 2000). In the older peatlands the concentration of Hg-polysulfides was insignificant due to the slightly lower pH. Furthermore, the significant correlations between the modeled concentrations of Hg-polysulfides and the net MeHg formation proxies MeHg and %MeHg in peat soil (Fig. S4c, d) also suggest an important role for polysulfides in net MeHg formation along the peatland chronosequence.

It should be noted that the formation of polysulfides requires the presence of elemental S in soils (Table S5). In a previous study that included a peatland similar to the older class of peatlands in the present study, elemental S was found at all sampled depths down to 25 cm (Liem-Nguyen et al., 2017). Thus, we expect S^0(s) to be present in the older peats of the chronosequence, but also in the younger peatlands where the S content is higher.

The Hg(II) speciation modeling also suggested less HgS (s) formation in the young peatland samples where the concentration of NOM−RS_{TOT} (ads, aq) functional groups was higher (Table S4), favoring these groups over HS^- in the competition for Hg(II) complexation in both aqueous and solid phases of the soil. As a consequence, HgS(s) was less prone to precipitate in the young peatlands (on average, around 6% of the total Hg(II) pool in soil, as compared to 20% in the old and 28% in the intermediate peatlands, Table S4). Together with Hg-polysulfide formation, this explains the relatively high solubility of Hg(II) in the young peatlands, despite having a smaller Hg(II) pool than the old peatlands (Fig. 2), possibly contributing to making more of the Hg(II) bioavailable in the young peatlands.

The performance of the thermodynamic chemical speciation model was improved, especially for the intermediate and young peatland samples, by the inclusion of HgS(s) precipitation and Hg(II)-polysulfide formation, but there was still a tendency to underpredict the concentration of Hg(II) in porewater (Fig. 7). One possible reason for a slightly less good fit for the intermediate and young peatland samples is that the concentration of NOM−RS_{TOT} functional groups was estimated using a fixed percentage of total S content. Thus, as a consequence of the 25% higher soil S content in the young peatland samples, the concentrations of NOM−RS_{TOT} were enhanced by 25% (0.015 mmol/g C for the young peatland samples compared to 0.012 mmol/g C for the old peatland samples; Table S4). This estimate was derived from data on soil samples from the SKM site studied by Liem-Nguyen et al. (2017), which can be considered to best reflect the old peatlands of the chronosequence. The assumption of a fixed ratio of NOM−RS_{TOT} to S_{TOT} along the peatland gradient may be an oversimplification though. In previous studies of forest organic soils and humic waters (Qian et al., 2002; Skyllberg et al., 2006) from the region, the NOM−RS_{TOT} was determined using the same method (Hg EXAFS) as in this study. This form corresponded to 20–30% of Org-S_{RED}, and 13–20 % of S_{TOT}. This is somewhat higher than our estimate of NOM−RS_{TOT} contributing to 15% of Org-S_{RED} and 9.8 % of S_{TOT}. Apart from variability in the redox potential, influencing the proportion of reduced and oxidized organic S, the formation of iron sulfide minerals (mainly FeS_2 and FeS) would influence the ratio between NOM−RS_{TOT} and S_{TOT}. In a lake sediment from the old peatland part of the chronosequence in which FeS_2 and FeS were both present, NOM−RS_{TOT} made up 22% of Org-S_{RED}, but only 6.8 % of S_{TOT} (Skyllberg et al., 2021). From porewater data we can say that mackinawite, FeS_m, was not present in our soils, but we cannot say anything about the presence or absence of pyrite, FeS_2(s), which may have varied along the chronosequence, and thus biased our assumption of a constant NOM−RS_{TOT} to S_{TOT} ratio.

An interesting finding is that, similar to the study of Liem-Nguyen et al. (2017), a log K of 36.8 (Drott et al.,

2013) for the formation reaction of HgS(s) improved the fit of the model to low inorganic sulfide (S(-II) < 1 μM) samples significantly, as compared to when using the constant of 37.6 (Schwarzenbach and Widmer, 1963). In contrast, the latter value showed a much better fit to data in lake sediments from the same region as this study (Skyllberg et al., 2021). As discussed by Skyllberg et al. (2021), the FeS_m may act as a precursor and increase the crystallinity of β-HgS(s) phases, which in turn may lower the availability of Hg to methylating bacteria. Thus, the absence of FeS_m in the peatland soils of this study, as well as in the study of Liem-Nguyen et al. (2017), may therefore result in a less crystalline and more bioavailable form of HgS(s) than in lake sediments.

The MeHg, like Hg(II), was more soluble in the young and intermediate peatlands, as indicated by the higher MeHg log K_d, than in the old peatlands. Thus, similar to Hg(II) being more bioavailable for methylating bacteria in the young peatlands, relatively more of the peatland's MeHg may be available for uptake in the aquatic food web downstream of young (mesotrophic) peatlands, as compared to the older (oligotrophic) peatlands.

5. CONCLUSIONS

This study aimed to evaluate the importance of three biogeochemical influences: electron donors, electron acceptors and bioavailable Hg(II) on the net MeHg formation, as approximated by MeHg concentrations and %MeHg (of total Hg) in peat soil, along a peatland chronosequence. The chronosequence covered a gradient of nutrient/trophic status divided into three age classes: old (oligotrophic), intermediate (oligo-mesotrophic) and young (mesotrophic) peatlands.

The study included an experiment where vascular plants were removed to impose a reduction of electron donors assumed to be associated with root exudates from those living plants. Because the vascular plant removal did not affect net MeHg formation, low molecular mass organic acids (LMM OA:s) or other geochemical parameters, we conclude that fresh root exudates from vascular plants did not influence net MeHg formation along this chronosequence. We also conclude that other processes than instantaneous exudation from plants regulated the concentrations of LMM OA:s in the peat soil, since there were differences in these concentrations across the chronosequence. The net MeHg formation proxies MeHg and %MeHg increased in the order of old < intermediate < young and were paralleled by similar patterns for potential electron donors (LMM OA:s and DOC/DON ratio) as well as potential electron donors (Fe(III), sulfate and Mn). Because electron donors, electron acceptors, as well as acidity (pH) and plant community all were changing in parallel along the chronosequence, it is difficult to resolve which, if any, of these factors were more important than any other in the limitation of Hg net methylation. Our thermodynamic modeling approach indicated that, although total aqueous concentrations of Hg(II) did not change along the chronosequence, less HgS(s) precipitation and higher concentration of Hg (II)-polysulfides in the young peatlands may have increased the bioavailability of Hg at this end of the gradient.

A possibility is emerging from recent studies, including the incubation experiments on soils from this chronosequence (Hu et al., 2020), that the concept of a single limiting factor will not suffice to represent the complex community structures where multiple factors interact to mediate net MeHg formation. Our study has also revealed that even though it was difficult to alter this property by short term (days to months) additions of e-donors or acceptors, the longer term availability of these resources influences net MeHg formation as evidenced by the consistent patterns along the chronosequence. This suggests there can be time-lags in microbial community response to changes in resource supplies before net MeHg formation changes.

Declaration of Competing Interest

The authors declare that they have no known competing financial interests or personal relationships that could have appeared to influence the work reported in this paper.

ACKNOWLEDGMENTS

We would like to thank Tao Jiang, Liem Nguyen, Yu Song and Wei Zhu for their assistance in the laboratory, and Lucas Perreal, Camille Guyenot, Thibaut Imbert, Edward van Westrene, Marloes Arens, Mélissa Garsany, Laura Manteau, Jeanne Latour, Charles Sanseverino, Quan Zhou and Itziar Aguinaga Gil for the help with the sampling. This work was supported by the China Scholarship Council (CSC; NO. 201408520034, NO. 201508430285), the Sino-Swedish Mercury Management Research Framework (SMaReF: VR2013-6978), the National Natural Science Foundation of China (No. 41573078, 41303098 and 42077297) and the Swedish Research Council Formas (2016-00896).

APPENDIX A. SUPPLEMENTARY MATERIAL

Supplementary data to this article can be found online at https://doi.org/10.1016/j.gca.2021.06.010.

REFERENCES

Åkerblom S., Bishop K., Björn E., Lambertsson L., Eriksson T. and Nilsson M. B. (2013) Significant interaction effects from sulfate deposition and climate on sulfur concentrations constitute major controls on methylmercury production in peatlands. *Geochim. Cosmochim. Acta* **102**, 1–11.

Åkerblom S., Nilsson M. B., Skyllberg U., Björn E., Jonsson S., Ranneby B. and Bishop K. (2020) Formation and mobilization of methylmercury across natural and experimental sulfur deposition gradients. *Environ. Pollut.* **263** 114398.

AMAP (2011) AMAP Assessment 2011: Mercury in the Arctic. Arctic Monitoring and Assessment Programme (AMAP).

Benoit J. M., Gilmour C. C., Heyes A., Mason R. P. and Miller C. L. (2003) Geochemical and Biological Controls over Methylmercury Production and Degradation in Aquatic Ecosystems, *Biogeochemistry of Environmentally Important Trace Elements. American Chemical Society*, 262–297.

Benoit J. M., Gilmour C. C., Mason R. P. and Heyes A. (1999) Sulfide Controls on Mercury Speciation and Bioavailability to Methylating Bacteria in Sediment Pore Waters. *Environ. Sci. Technol.* **33**, 951–957.

Bergman I., Bishop K., Tu Q., Frech W., Akerblom S. and Nilsson M. (2012) The Influence of Sulphate Deposition on the Seasonal Variation of Peat Pore Water Methyl Hg in a Boreal Mire. *PLoS ONE* **7**, 10.

Bragazza L., Bardgett R. D., Mitchell E. A. D. and Buttler A. (2015) Linking soil microbial communities to vascular plant abundance along a climate gradient. *New Phytol* **205**, 1175–1182.

Branfireun B. A., Bishop K., Roulet N. T., Granberg G. and Nilsson M. (2001) Mercury cycling in boreal ecosystems: The long-term effect of acid rain constituents on peatland pore water methylmercury concentrations. *Geophys. Res. Lett.* **28**, 1227–1230.

Bravo A. G., Bouchet S., Tolu J., Björn E., Mateos-Rivera A. and Bertilsson S. (2017) Molecular composition of organic matter controls methylmercury formation in boreal lakes. *Nat. Commun.* **8**, 14255.

Cline J. D. (1969) Spectrophotometric determination of hydrogen sulfide in natural waters. *Limnol. Oceanogr.* **14**, 454–458.

Compeau G. C. and Bartha R. (1985) Sulfate-Reducing Bacteria: Principal Methylators of Mercury in Anoxic Estuarine Sediment. *Appl. Environ. Microbiol.* **50**, 498–502.

Driscoll C. T., Yan C., Schofield C. L., Munson R. and Holsapple J. (1994) The mercury cycle and fish in the Adirondack lakes. *Environ. Sci. Technol.* **28**, 136A–143A.

Drott A., Björn E., Bouchet S. and Skyllberg U. (2013) Refining Thermodynamic Constants for Mercury(II)-Sulfides in Equilibrium with Metacinnabar at Sub-Micromolar Aqueous Sulfide Concentrations. *Environ. Sci. Technol.* **47**, 4197–4203.

Drott A., Lambertsson L., Björn E. and Skyllberg U. (2008) Do Potential Methylation Rates Reflect Accumulated Methyl Mercury in Contaminated Sediments?. *Environ. Sci. Technol.* **42**, 153–158.

Gilmour C. C., Podar M., Bullock A. L., Graham A. M., Brown S. D., Somenahally A. C., Johs A., Hurt R. A., Bailey K. L. and Elias D. A. (2013) Mercury Methylation by Novel Microorganisms from New Environments. *Environ. Sci. Technol.* **47**, 11810–11820.

Gilmour C. C., Riedel G. S., Ederington M. C., Bell J. T., Gill G. A. and Stordal M. C. (1998) Methylmercury concentrations and production rates across a trophic gradient in the northern Everglades. *Biogeochemistry* **40**, 327–345.

Gordon J., Quinton W., Branfireun B. A. and Olefeldt D. (2016) Mercury and methylmercury biogeochemistry in a thawing permafrost wetland complex, Northwest Territories, Canada. *Hydrol. Process.* **30**, 3627–3638.

Graham A. M., Cameron-Burr K. T., Hajic H. A., Lee C., Msekela D. and Gilmour C. C. (2017) Sulfurization of Dissolved Organic Matter Increases Hg–Sulfide–Dissolved Organic Matter Bioavailability to a Hg-Methylating Bacterium. *Environ. Sci. Technol.* **51**, 9080–9088.

Hamelin S., Amyot M., Barkay T., Wang Y. and Planas D. (2011) Methanogens: principal methylators of mercury in lake periphyton. *Environ Sci Technol* **45**, 7693–7700.

Hoggarth C. G. J., Hall B. D. and Mitchell C. P. J. (2015) Mercury methylation in high and low-sulphate impacted wetland ponds within the prairie pothole region of North America. *Environ. Pollut.* **205**, 269–277.

Hu H., Wang B., Bravo A. G., Björn E., Skyllberg U., Amouroux D., Tessier E., Zopfi J., Feng X., Bishop K., Nilsson M. B. and Bertilsson S. (2020) Shifts in mercury methylation across a peatland chronosequence: From sulfate reduction to methanogenesis and syntrophy. *J. Hazard. Mater.* **387** 121967.

Jay J. A., Morel F. M. M. and Hemond H. F. (2000) Mercury Speciation in the Presence of Polysulfides. *Environ. Sci. Technol.* **34**, 2196–2200.

Jensen S. and Jernelöv A. (1969) Biological Methylation of Mercury in Aquatic Organisms. *Nature* **223**, 753.

Jeremiason J. D., Engstrom D. R., Swain E. B., Nater E. A., Johnson B. M., Almendinger J. E., Monson B. A. and Kolka R. K. (2006) Sulfate Addition Increases Methylmercury Production in an Experimental Wetland. *Environ. Sci. Technol.* **40**, 3800–3806.

Jing M., Lin D., Wu P., Kainz M. J., Bishop K., Yan H., Wang R., Wang Q. and Li Q. (2020) Effect of aquaculture on mercury and polyunsaturated fatty acids in fishes from reservoirs in Southwest China. *Environ. Pollut.* **257** 113543.

Jonsson S., Skyllberg U., Nilsson M. B., Lundberg E., Andersson A. and Björn E. (2014) Differentiated availability of geochemical mercury pools controls methylmercury levels in estuarine sediment and biota. *Nat. Commun.* **5**, 4624.

Keller J. K., Sutton-Grier A. E., Bullock A. L. and Megonigal J. P. (2013) Anaerobic Metabolism in Tidal Freshwater Wetlands: I. Plant Removal Effects on Iron Reduction and Methanogenesis. *Estuaries Coasts* **36**, 457–470.

Kronberg R.-M., Tjerngren I., Drott A., Björn E. and Skyllberg U. (2012) Net Degradation of Methyl Mercury in Alder Swamps. *Environ. Sci. Technol.* **46**, 13144–13151.

Laine A. M., Lindholm T., Nilsson M., Kutznetsov O., Jassey V. E. J. and Tuittila E.-S. (2021) Functional diversity and trait composition of vascular plant and Sphagnum moss communities during peatland succession across land uplift regions. *J Ecol* **109**, 1774–1789.

Lambertsson L. and Björn E. (2004) Validation of a simplified field-adapted procedure for routine determinations of methyl mercury at trace levels in natural water samples using species-specific isotope dilution mass spectrometry. *Anal. Bioanal. Chem.* **380**, 871–875.

Langer C. S., Fitzgerald W. F., Visscher P. T. and Vandal G. M. (2001) Biogeochemical cycling of methylmercury at Barn Island Salt Marsh, Stonington, CT, USA. *Wetlands Ecol. Manage.* **9**, 295–310.

Li Y., Zhao J., Zhong H., Wang Y., Li H., Li Y.-F., Liem-Nguyen V., Jiang T., Zhang Z., Gao Y. and Chai Z. (2019) Understanding enhanced microbial MeHg production in mining-contaminated paddy soils under sulfate amendment: Changes in Hg mobility or microbial methylators?. *Environ. Sci. Technol.* **53**, 1844–1852.

Liem-Nguyen V., Skyllberg U. and Björn E. (2017) Thermodynamic Modeling of the Solubility and Chemical Speciation of Mercury and Methylmercury Driven by Organic Thiols and Micromolar Sulfide Concentrations in Boreal Wetland Soils. *Environ. Sci. Technol.* **51**, 3678–3686.

Liu P. and Conrad R. (2017) Syntrophobacteraceae-affiliated species are major propionate-degrading sulfate reducers in paddy soil. *Environ. Microbiol.* **19**, 1669–1686.

Loseto L. L., Siciliano S. D. and Lean D. R. (2004) Methylmercury production in High Arctic wetlands. *Environ Toxicol Chem* **23**, 17–23.

Macdonald R. W., Harner T. and Fyfe J. (2005) Recent climate change in the Arctic and its impact on contaminant pathways and interpretation of temporal trend data. *Sci. Total Environ.* **342**, 5–86.

Millero F. J., Plese T. and Fernandez M. (1988) The dissociation of hydrogen sulfide in seawater1. *Limnol. Oceanogr.* **33**, 269–274.

Mitchell C. P. J., Branfireun B. A. and Kolka R. K. (2008a) Assessing sulfate and carbon controls on net methylmercury

production in peatlands: An in situ mesocosm approach. *Appl. Geochem.* **23**, 503–518.
Mitchell C. P. J., Branfireun B. A. and Kolka R. K. (2008b) Spatial Characteristics of Net Methylmercury Production Hot Spots in Peatlands. *Environ. Sci. Technol.* **42**, 1010–1016.
Munthe J., Bodaly R. A., Branfireun B. A., Driscoll C. T., Gilmour C. C., Harris R., Horvat M., Lucotte M. and Malm O. (2007) Recovery of mercury-contaminated fisheries. *Ambio* **36**, 33–44.
Poulin B. A., Ryan J. N., Tate M. T., Krabbenhoft D. P., Hines M. E., Barkay T., Schaefer J. and Aiken G. R. (2019) Geochemical Factors Controlling Dissolved Elemental Mercury and Methylmercury Formation in Alaskan Wetlands of Varying Trophic Status. *Environ. Sci. Technol.* **53**, 6203–6213.
Qian J., Skyllberg U., Frech W., Bleam W. F., Bloom P. R. and Petit P. E. (2002) Bonding of methyl mercury to reduced sulfur groups in soil and stream organic matter as determined by x-ray absorption spectroscopy and binding affinity studies. *Geochim. Cosmochim. Acta* **66**, 3873–3885.
Ratcliffe H. E., Swanson G. M. and Fischer L. J. (1996) Human exposure to mercury: a critical assessment of the evidence of adverse health effects. *Journal of toxicology and environmental health* **49**, 221–270.
Ravichandran M., Aiken G. R., Ryan J. N. and Reddy M. M. (1999) Inhibition of Precipitation and Aggregation of Metacinnabar (Mercuric Sulfide) by Dissolved Organic Matter Isolated from the Florida Everglades. *Environ. Sci. Technol.* **33**, 1418–1423.
Renberg I. and Segerström U. (1981) The initial points on a shoreline displacement curve for southern Västerbotten, dated by varve-counts of lake sediments. In *Florilegium Florins Dedicatum* (eds. L.-. K. Königsson and K. Paabo). Striae, Uppsala, pp. 174–176.
Rickard D. (2006) The solubility of FeS. *Geochim. Cosmochim. Acta* **70**, 5779–5789.
Schwarzenbach G. and Widmer M. (1963) Die Löslichkeit von Metallsulfiden I. *Schwarzes Quecksilbersulfid. Helvetica Chimica Acta* **46**, 2613–2628.
Si Y., Zou Y., Liu X., Si X. and Mao J. (2015) Mercury methylation coupled to iron reduction by dissimilatory iron-reducing bacteria. *Chemosphere* **122**, 206–212.
Skyllberg U. (2012) Chemical Speciation of Mercury in Soil and Sediment, in: Liu, G., Cai, Y., O'Driscoll, N.J. (Eds.), Environmental Chemistry and Toxicology of Mercury, pp. 219-258.
Skyllberg U., Bloom P. R., Qian J., Lin C.-M. and Bleam W. F. (2006) Complexation of Mercury(II) in Soil Organic Matter: EXAFS Evidence for Linear Two-Coordination with Reduced Sulfur Groups. *Environ. Sci. Technol.* **40**, 4174–4180.
Skyllberg U., Persson A., Tjerngren I., Kronberg R.-M., Drott A., Meili M. and Björn E. (2021) Chemical speciation of mercury, sulfur and iron in a dystrophic boreal lake sediment, as controlled by the formation of mackinawite and framboidal pyrite. *Geochim. Cosmochim. Acta* **294**, 106–125.
Skyllberg U., Westin M. B., Meili M. and Björn E. (2009) Elevated Concentrations of Methyl Mercury in Streams after Forest Clear-Cut: A Consequence of Mobilization from Soil or New Methylation?. *Environ. Sci. Technol.* **43**, 8535–8541.
Spangler W. J., Spigarelli J. L., Rose J. M. and Miller H. M. (1973) Methylmercury: Bacterial Degradation in Lake Sediments. *Science* **180**, 192–193.
St. Louis V.L., Rudd J.W.M., Kelly C.A., Beaty K.G., Flett R.J. and Roulet N.T. (1996) Production and Loss of Methylmercury and Loss of Total Mercury from Boreal Forest Catchments Containing Different Types of Wetlands. Environ. Sci. Technol. 30, 2719-2729.
Strandberg U., Palviainen M., Eronen A., Piirainen S., Laurén A., Akkanen J. and Kankaala P. (2016) Spatial variability of mercury and polyunsaturated fatty acids in the European perch (Perca fluviatilis) – Implications for risk-benefit analyses of fish consumption. *Environ. Pollut.* **219**, 305–314.
Tjerngren I., Karlsson T., Bjorn E. and Skyllberg U. (2012a) Potential Hg methylation and MeHg demethylation rates related to the nutrient status of different boreal wetlands. *Biogeochemistry* **108**, 335–350.
Tjerngren I., Meili M., Bjorn E. and Skyllberg U. (2012b) Eight Boreal Wetlands as Sources and Sinks for Methyl Mercury in Relation to Soil Acidity, C/N Ratio, and Small-Scale Flooding. *Environ. Sci. Technol.* **46**, 8052–8060.
Tuittila E.-S., Juutinen S., Frolking S., Väliranta M., Laine A. M., Miettinen A., Seväkivi M.-L., Quillet A. and Merilä P. (2013) Wetland chronosequence as a model of peatland development: Vegetation succession, peat and carbon accumulation. *The Holocene* **23**, 25–35.
Villinski J. E., O'Day P. A., Corley T. L. and Conklin M. H. (2001) In Situ Spectroscopic and Solution Analyses of the Reductive Dissolution of MnO2 by Fe(II). *Environ. Sci. Technol.* **35**, 1157–1163.
Viollier E., Inglett P. W., Hunter K., Roychoudhury A. N. and Van Cappellen P. (2000) The ferrozine method revisited: Fe(II)/Fe(III) determination in natural waters. *Appl. Geochem.* **15**, 785–790.
Wang B., Nilsson M. B., Eklöf K., Hu H., Ehnvall B., Bravo A. G., Zhong S., Åkeblom S., Björn E., Bertilsson S., Skyllberg U. and Bishop K. (2020) Opposing spatial trends in methylmercury and total mercury along a peatland chronosequence trophic gradient. *Sci. Total Environ.* **718** 137306.
Weishaar J. L., Aiken G. R., Bergamaschi B. A., Fram M. S., Fujii R. and Mopper K. (2003) Evaluation of Specific Ultraviolet Absorbance as an Indicator of the Chemical Composition and Reactivity of Dissolved Organic Carbon. *Environ. Sci. Technol.* **37**, 4702–4708.
Windham-Myers L., Marvin-Dipasquale M., Krabbenhoft D. P., Agee J. L., Cox M. H., Heredia-Middleton P., Coates C. and Kakouros E. (2009) Experimental removal of wetland emergent vegetation leads to decreased methylmercury production in surface sediment. *Journal of Geophysical Research. Biogeosciences* **114**, G00C05.
Yu R.-Q., Reinfelder J. R., Hines M. E. and Barkay T. (2018) Syntrophic pathways for microbial mercury methylation. *The ISME Journal* **12**, 1826–1835.
Zhu W., Song Y., Adediran G. A., Jiang T., Reis A. T., Pereira E., Skyllberg U. and Björn E. (2018) Mercury transformations in resuspended contaminated sediment controlled by redox conditions, chemical speciation and sources of organic matter. *Geochim. Cosmochim. Acta* **220**, 158–179.

Associate editor: Brandy Marie Toner